Biochimica et Biophysica Acta 1797 (2010) 272–277

Contents lists available at ScienceDirect

Biochimica et Biophysica Acta

journal homepage: www.elsevier.com/locate/bbabio

Row-like organization of ATP synthase in intact mitochondria determined by cryo-electron tomography

Natalya V. Dudkina [a], Gert T. Oostergetel [a], Dagmar Lewejohann [b], Hans-Peter Braun [b], Egbert J. Boekema [a,*]

[a] Electron microscopy group, Groningen Biomolecular Sciences and Biotechnology Institute, University of Groningen, Groningen, The Netherlands
[b] Institute for Plant Genetics, Faculty of Natural Sciences, Leibniz Universität Hannover, Hannover, Germany

ARTICLE INFO

Article history:
Received 22 September 2009
Received in revised form 4 November 2009
Accepted 6 November 2009
Available online 17 November 2009

Keywords:
ATP synthase
Electron tomography
Mitochondria
Polytomella

ABSTRACT

The fine structure of intact, close-to-spherical mitochondria from the alga *Polytomella* was visualized by dual-axis cryo-electron tomography. The supramolecular organization of dimeric ATP synthase in the cristae membranes was investigated by averaging subvolumes of tomograms and 3D details at ~6 nm resolution were revealed. Oligomeric ATP synthase is composed of rows of dimers at 12 nm intervals; the dimers make a slight angle along the row. In addition, the main features of monomeric ATP synthase, such as the conically shaped F_1 headpiece, central stalk and stator were revealed. This demonstrates the capability of dual-axis electron tomography to unravel details of proteins and their interactions in complete organelles.

1. Introduction

Mitochondria play a central role in the eukaryotic energy metabolism. They are surrounded by an outer membrane acting as a barrier for larger macromolecules (>5 kDa) and an inner membrane which encloses the matrix space where abundant micro-compartments named cristae are present. The cristae membrane is highly enriched with oxidative phosphorylation (OXPHOS) complexes and ATP synthase molecules. Most of the recent knowledge about the mitochondrial ultrastructure has been provided by (cryo)-electron tomography (ET) [1–5]. Cryo-ET is an emerging electron microscopic technique for reconstructing 3D volumes by incremental tilting and imaging the specimen in discrete steps over a relatively large range of angles around a tilt axis under cryogenic conditions.

ET has revealed that the cristae are connected to the inner membrane by narrow tubular junctions, which likely restrict diffusion. ET also strongly suggests that the inner membrane topology represents a balance between membrane fusion and fission processes [4]. The resolution of ET is directly related to the size of the object [6] and for an organelle like the mitochondrion it can be in the range of 6–10 nm. At this resolution the larger protein complexes are detectable in tomograms by pattern recognition and subvolumes can be selected and averaged. This has been recently shown for ribosomes [7] and polysomes [8]. The visualization of proteins within quickly frozen mitochondria without chemical fixatives makes ET a very attractive method to study the native higher organization of protein complexes in the cytosol or membrane.

The supramolecular organization of the OXPHOS complexes within the abundant cristae is a topic that has been studied in several ways. Until the mid-1990s they were considered to exist as single copies, closely packed in the membranes. First evidence for a dimeric organization of ATP synthase complexes in the mitochondrial inner membrane came from the work of Arnold and coworkers [9]. They characterized dimeric ATP synthases by blue-native gel electrophoresis (BN-PAGE). Recently, dimeric ATP synthases from bovine [10], *Polytomella* [11] and *S. cerevisiae* [12] were characterized by single particle electron microscopy, leaving little doubt for their existence. Dimeric ATP synthases were suggested to be the building blocks of the oligomeric rows of ATP synthases in the tubular cristae as it was described by BN-PAGE [13]. Indeed, a row-like arrangement of ATP synthase was previously demonstrated on deep-etched specimens by electron microscopy [14] and recently by cryo-ET [15]. The oligomeric chains were proposed to induce the local curvature of the inner mitochondrial membrane [10,11] which would then enhance the local proton gradient necessary for ATP synthesis [15].

Mitochondrial F_1F_0 ATP synthase is a complex of 600 kDa formed by 15–18 subunits [16,17]. The matrix-exposed F_1 part is connected to the membrane-embedded hydrophobic F_0 part via a central stalk and a peripheral stalk plus the OSCP subunit. In this study we focus on ATP synthase from the colorless green alga *Polytomella*, a close relative of *Chlamydomonas*, because of its highly stable dimers. Recently it was demonstrated that the *Polytomella* enzyme lacks the classical subunits which constitute the peripheral stalk and those involved in the dimerization of mammalian and fungal complexes. Instead, it contains 9 unique subunits called ASA1 to 9 [18].

Until recently only single-axis cryo-ET was possible due to technical limitations but a breakthrough came with the development

* Corresponding author. Tel.: +31 0 50 3634225; fax: +31 0 50 363 4800.
E-mail address: e.j.boekema@rug.nl (E.J. Boekema).

0005-2728/$ – see front matter © 2009 Elsevier B.V. All rights reserved.
doi:10.1016/j.bbabio.2009.11.004

of the flip-flop rotation stage allowing to collect two orthogonal tilt series in a cryo-protected way [19]. Dual-axis tilting reduces the missing information of sampling originating from single-axis tilting over restricted tilt angles. In 3D space, the missing wedge is reduced to a missing pyramid, which results in a more isotropic sampling of the volume. Because the knowledge about the overall organization of mitochondrial proteins is still at its infancy we used dual-axis cryo-ET to study the supramolecular organization of OXPHOS complexes in *Polytomella* mitochondria. A special quality of *Polytomella* mitochondria is the high abundance of dimeric ATP synthase. We were able to reconstruct complete mitochondria of ~0.5–1.5 μm in size. The supramolecular organization of dimeric ATP synthase was visualized by averaging subvolumes of tomograms. We obtained 3D details at ~6 nm resolution which reveal not only the interaction within dimers, but also the main features of monomeric ATP synthase. This study demonstrates the capability of dual-axis ET to unravel the details of proteins and their interactions within reconstructions of complete organelles.

2. Materials and methods

2.1. Preparation of mitochondria

Mitochondria from *Polytomella* cultures were isolated by differential centrifugation and Percol density gradient centrifugation as described before [11]. Oxygen consumption measurements of mitochondria (10 mg organelles in 0.3 M mannitol, 10 mM K_2HPO_4 [pH 7.2], 10 mM KCl, 5 mM $MgCl_2$) were carried out using a Clark-type oxygen electrode in a reaction chamber of 2 ml. State I to IV respiration was determined by successively adding succinate (15 mM), ADP (5 mM), KCN (5 mM), and salicylhydroxamic acid (7.5 mM).

2.2. Cryo-electron tomography

Freshly isolated mitochondria were mixed with 10-nm gold particles as fiducial markers and 2.5μl was applied to glow-discharged 200 mesh Quantifoil specimen support grids (Quantifoil Micro Tools GmbH) and vitrified in liquid ethane using a Vitrobot Mk3 (FEI). Grids were blotted in a 100% humidified atmosphere for 3 s at a blot offset (the longitudinal grid positioning) setting of −3.5. ET was performed on a 300 kV G2 Polara electron microscope (FEI) equipped with a Gatan post-column energy filter. Images were recorded with a 2k×2k CCD camera (Gatan) at 10 μm underfocus (first CTF zero at 4.0 nm) and 41,400× magnification, resulting in a pixel of 0.725 nm at the level of the specimen. Dual-axis tilt series were recorded at 2° increments with a total dose of about 8000 electrons/nm^2.

2.3. 3D reconstruction and image analysis

Tomograms were calculated using IMOD software [20]. For final tomograms the volumes derived from the two single-axis tilts were aligned to each other and combined and denoised with 20 iterations by non-linear anisotropic diffusion [21]. Averaging of manually selected subvolumes with a box size of 120×120×120 pixels from 15 reconstructed mitochondria was done with PEET programs as a part of the IMOD package. The resolution of the final reconstruction was estimated by Fourier Shell Correlation [22] at 0.3 threshold with EMAN software [23].

2.4. Cryo-electron microscopy and analysis

Dimeric ATP synthase was purified by blue-native polyacrylamide gel electrophoresis (BN-PAGE) [24] and extracted from gels by electroelution. Starting material for BN-PAGE separations was 10 mg mitochondrial proteins which were loaded into 10 wells of a 16×16×0.15 mm polyacrylamide gel. Protein separation took place in the Protean-II chamber (Biorad, München, Germany) at constant voltage (500 V) for 12 h. Electroelution was carried out using an electroeluter from C.B.S. Scientific (Del Mar, CA, USA) in electroelution buffer (25 mM Tricine, 7.5 mM Bis–Tris and 0.01% digitonin) at 150 V and 4 °C overnight according to the manufacturer's instructions. Aliquots of purified ATP synthase were applied to glow-discharged 400 mesh Quantifoil support grids covered with a thin additional carbon layer and quickly frozen by plunging into liquid ethane using a Vitrobot. Data were collected on a 300 kV G2 Polara electron microscope at 1.5–2.5 μm underfocus and 78,000× magnification, at a pixel size of 0.38 nm. Because at these underfocus values all image details up to 2.2 nm resolution are imaged with the correct positive phase value, no contrast

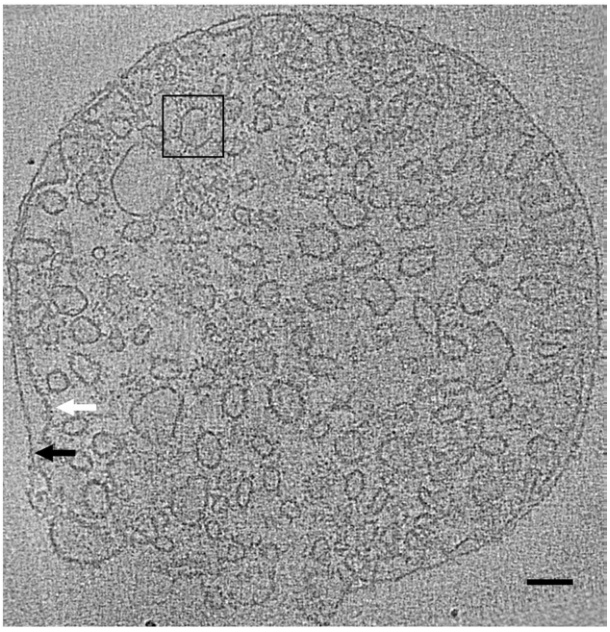

Fig. 1. Cryo-EM tomography of a full mitochondrion from *Polytomella*. A slice through the center shows the outer membrane (black arrow) and the folded thicker inner membrane (white arrow) and multiple cristae inside. The square box shows a cristae membrane part with clearly visible protruding F_1-headpieces of ATP synthase complexes. Scale bar, 100 nm.

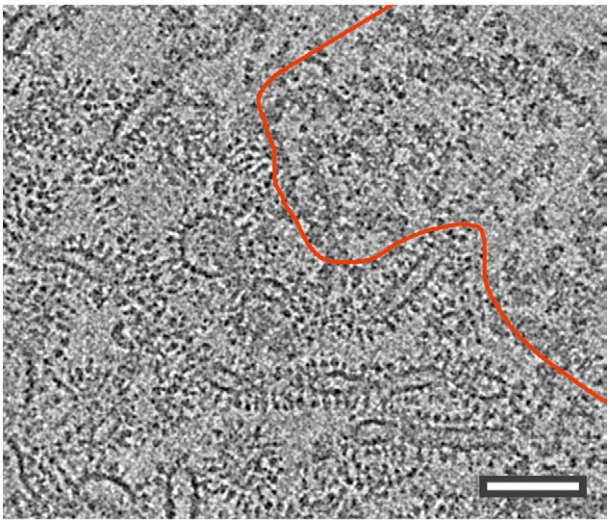

Fig. 2. Selected part of a cryo-EM tomogram showing a slice with a strong separation between areas occupied with cristae (below red line) and areas devoid of cristae but packed with large densities, supposed to represent ribosomes and or other components of the protein synthesis machinery (above red line). Scale bar, 100 nm.

transfer function (CTF) correction was performed. Single particle image analysis was performed with GRIP software [11].

3. Results

Starting point of dual-axis cryo-ET analyses was mitochondria freshly isolated from a *Polytomella* culture. Purified organelles had oxygen consumption rates of 10 nmol/mg protein/minute. Intactness of the purified organelles was further confirmed by structural investigations. In generated tomograms mitochondria are represented as close-to-spherical organelles of 0.5–1.5 μm in size, but because we used ice layers with a thickness of ~0.5 μm, they were somewhat flattened or oriented with their smallest dimension vertically. They were surrounded by an outer and inner membrane (Fig. 1, white and black arrows), but experiments demonstrated that the outer membrane was mostly disrupted unless fresh material was used. Fig. 1 shows a mitochondrion surrounded by a double-membrane indicating that this organelle is intact. Distribution of the inner content of mitochondria varied between the 15 different reconstructions. In some mitochondria the cristae are evenly distributed and about spherical (Fig. 1 and supplementary data), in others they are more tubular and/or clustered. If the cristae are clustered, there are also regions which are completely free of any membrane. Membrane-free areas have a higher average density than the immediate surrounding of the cristae and are likely containing densely packed material which could represent ribosomes and other components of the protein synthesis machinery including the DNA nucleoids (Fig. 2). In the rest of the study we have focused on the cristae.

Close examination of tomograms reveals that cristae are abundantly coated with large membrane-bound proteins running in two parallel rows, which are likely the F_1-heads of ATP synthases (Fig. 3A). Since averaging of electron microscopy 2D and 3D data enhances the signal considerably, averaging of tomogram subvolumes was performed. We selected 550 subvolumes of potentially oligomeric ATP

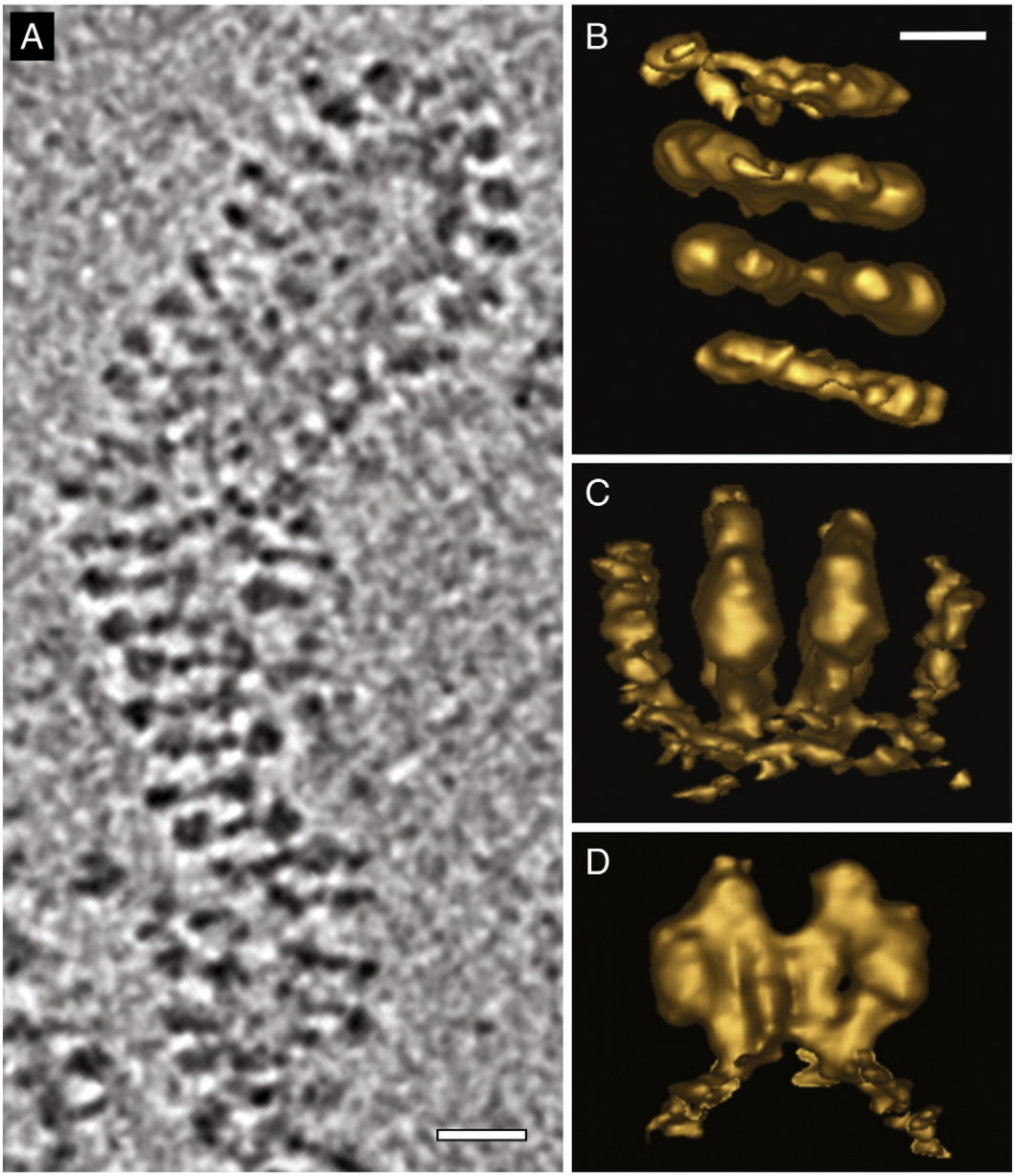

Fig. 3. (A) A complete tubular cristae, with a row of ATP synthase dimers in the lower half, seen from the top. (B) Average image of 166 tomographic subvolumes of oligomeric ATP synthase from the top. The image shows about half of the volume of 120 pixels. (C) Averaged tomographic subvolume of dimeric ATP synthase seen from aside, displayed with a lower density cutoff to visualize the membrane. (D) Central dimer displayed at low density cutoff as in C, 90° rotated vertically. Scale bar for frame A, 20 nm; bar for B–D, 10 nm.

synthases within a box size of 120×120×120 pixels, equivalent to 87×87×87 nm. An average of 166 well-aligned subvolumes has a resolution of 5.7 nm and shows rows of dimeric ATP synthase at 12 nm intervals (Fig. 3B). The row is not a straight line of dimers, because there is a slight angle between them along the row. From a view perpendicular to the row it appears that the central dimers make an angle of 9° with respect to each other.

To get a full assignment of the averaged tomograms as dimeric ATP synthase a comparison with previously performed single particle averaging on negatively stained dimers is useful (Fig. 4B). In addition, we analyzed unstained, purified ATP synthase in a thin layer of amorphous ice on carbon support films (see Section 2.4). Only one type of projection was obtained, in which the ATP synthase dimer is seen from the top (Fig. 4D). If we now compare the two views from single particle analysis with similar views generated from the averaged 3D volume it is obvious that the latter resembles the purified dimer in negative stain well (Fig. 4B). Common features are the water-soluble F_1-part ("F_1", Fig. 4A), the central stalk (C), the membrane-embedded F_0 part (F_0), the connecting stalk or stator (S) and the massive density "A" of the peripheral stalk next to the headpiece, assigned to the *Polytomella*-unique ASA1 subunit [25]. The finest resolved detail is the site where the stator connects to the OSCP subunit (Fig. 4A, B, yellow arrows). The membrane F_0 part looks more bulky in negative stain, which is due to the presence of a detergent boundary layer, necessary to keep the molecules in a monodisperse state in solution (blue arrows, Fig. 4A, B). It is known that the detergent layer around purified membrane proteins in negatively stained EM samples can increase the particle dimensions substantially [26]. The membrane part is not fully present in the averaged tomographic volume, probably because of the lower density of the lipids in comparison to the protein (Fig. 4A). The reconstruction is presented with a volume of ~900 nm^3 for the α3β3γ-OSCP moiety of the headpiece, according to the high-resolution X-ray structure [16]. If displayed at a lower density cutoff, the position of the membrane becomes visible (Fig. 3D). The ATP synthase dimers have been postulated to induce a local curvature of the membrane [10,11]; ET now shows that the curvature is close to 90°. Monomeric ATP synthases contact mostly via the membrane F_0-parts and to some extent by the peripheral stalks. The monomers make an angle of ~70° within the dimer, resembling the medium-resolution 2D map in negative stain by single particle image analysis (Fig. 4B). The positions of the peripheral stalk and the ASA1 domain in 3D dimer volume correspond to those in the 2D single particle top-view projection (Fig. 4C, D, green lines). It is not clear how the dimers are connected in the oligomeric chain via the membrane parts. No inter-dimer interaction is visible between the headpieces and between peripheral stalks. The location of the other OXPHOS complexes, and other large structures, like ribosomes was not further investigated, but considering the resolution it should be possible to search for some of these by searching software known as template matching [7]. On the other hand, the *Polytomella* ribosome has not been structurally investigated yet.

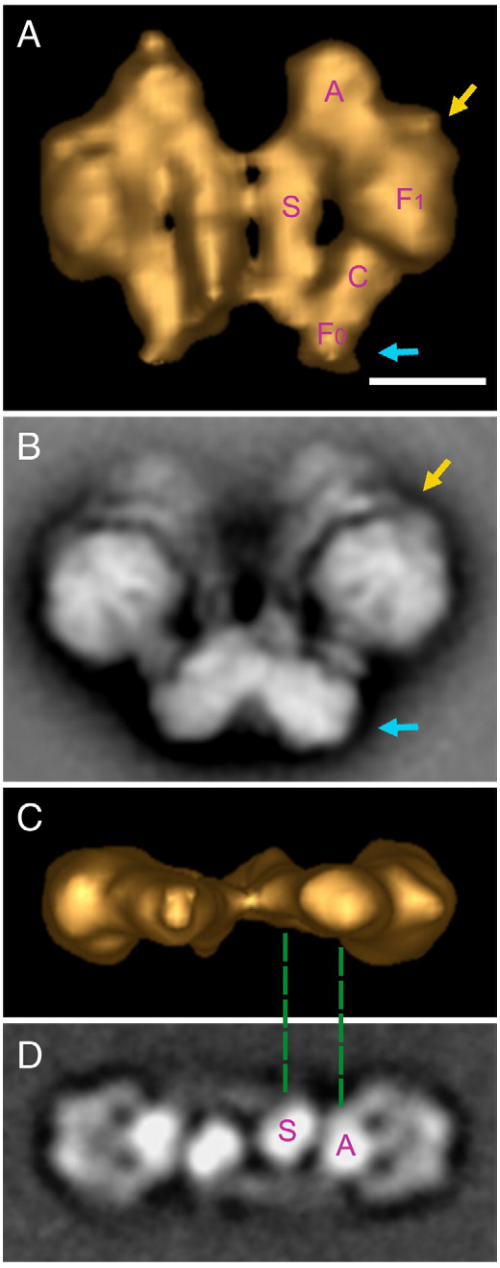

Fig. 4. Further analysis of ATP synthase subvolume and comparison. (A) Averaged dimer volume of ATP synthase from frame of Fig. 3D (second from below) at higher density cutoff from a side. (B) Negatively stained side view of dimeric ATP synthase (reproduced from [11]. (C) Averaged subvolume of dimeric ATP synthase from the top. (D) Average of 1024 2D top-view projections of isolated ATP synthase dimer originating from the single particle cryo-EM. A — ASA1 subunit, S — stator, C — central stalk, F_1 — headpiece, F_0 — membrane domain. Yellow arrows mark the connection between the OSCP subunit of the F_1 part and the stator; blue arrows mark the site where the detergent shell is absent (frame A) or present (frame B); green lines highlight similarities of the tomographic reconstruction and the cryo-2D map concerning the position of the stator and ASA1 domain. Scale bar, 10 nm.

4. Discussion

We have obtained 3D reconstructions of intact mitochondria by cryo-ET and averaged 3D subvolumes of oligomeric ATP synthase at 5.7 nm resolution. This reveals the 3D arrangement of ATP synthase dimer rows within the cristae membranes. Specific known details of monomeric ATP synthase were revealed for the first time in intact organelles, such as the conically shaped headpiece, the connection of the stator to the OSCP subunit right on top of the F_1 headpiece, the central stalk and the fixed angle of ~70° between monomers (Fig. 4A). The fact that these features appear as expected from medium-resolution single particle image analysis in negative stain (Fig. 4B) [11] and in accordance with the high-resolution X-ray model [17], indicates that the inter-dimer interactions of the oligomers must be real features as well. The 3D tomography data indicate that the peripheral stalks of the monomers are in close contact, which probably limits their mobility. This observation has an implication for the mechanism of the enzyme. At least one flexible part in the ATP synthase molecule is required to store transient energy during the stepping rotation of the central stalk. The obvious candidate for elastic energy storage is the α-helical region of the γ-subunit in the central stalk (see [27] for a discussion). But it has also been suggested many times that the peripheral stalk could store elastic energy as

well (see [28] for a review). The fact that peripheral stalks of the monomers interact makes it less likely that they are involved in storing transient energy.

We now directly visualized the local curvature of the membrane around ATP synthase dimers, which appears to be as much as 90° in a direction perpendicular to the rows (Fig. 3D). The ATP synthase dimers show also some curvature in the long direction of the rows because the central dimers make an angle with each other (Fig. 3C), but if this has some effect on the level of the cristae membrane is not clear. The precise amount of curvature between the dimers along the rows could not be investigated, because in the averaged 3D subvolume the peripheral dimers of the row appear more fuzzy than the inner ones. Fuzziness is likely caused by an angular variation between dimers. In analyzing 2D maps of large multi-subunit complexes we have noticed several times a local fuzziness in structures, indicating flexibilities in attachments of components [29].

Multimeric ATP synthase was previously found, but with less detail. At a time that mitochondrial ATP synthase was not yet considered to be dimeric, it was demonstrated in frozen, deep-etched *Paramecium* mitochondria that double rows of ATP synthases exist on tubular-shaped cristae [14]. A recent cryo-ET investigation of bovine and rat mitochondrial membranes revealed that ATP synthases run as dimer ribbons in a kinked, inner membrane [15]. The collected data indicate that oligomeric organization of ATP synthases in the inner mitochondrial membrane might be a common feature in different organisms.

Our data demonstrate that monomers interact not only via the membrane F_0 parts, as it was shown before, but that the peripheral stalks are also involved. This intensified connection increases the stability of the dimer. The measured angle of 70° between the two F_1F_0 ATP synthases in intact mitochondria strongly points at a functional role of ATP synthases in the curvature of the inner mitochondrial membrane. It is likely that the membrane curvature is caused by adapting the shape of the curved dimers, rather than that a curved membrane induces a kink in the ATP synthase dimers. The fact that isolated dimers retain their shape strongly points to an active role in shaping the cristae.

The question remains where the other OXPHOS (super)complexes are localized. Strauss and colleagues [15] proposed in their work on mammalian mitochondria that they occupy the less highly curved regions. In the case of *Polytomella* almost all cristae are tubular-shaped and densely packed with ATP synthases. We consider OXPHOS complexes in *Polytomella* to be present in smaller numbers located between the rows of ATP synthases and/or in less-curved membrane areas. The final answer requires further research, but likely also a higher resolution than achievable with current equipment (see last sections). Dimeric complex III (500 kDa) and monomeric complex IV (200 kDa) are currently too small to be picked up by template matching [7], but assigning positions of larger supercomplexes, consisting of complex I (1000 kDa) and III or I + III + IV might be possible, if such complexes are present.

Our investigation of oligomeric ATP synthase in *Polytomella* is one of the first applications of dual-axis cryo-ET on intact organelles. The elements of the ATP synthase dimers are well resolved, if compared with those of bovine and rat mitochondria from single-axis tomography [15]. The bovine resolution that we measured for our reconstruction is lower than the value presented in [15], the visibility of substantially more details in the structure presented here points to a higher resolution obtained in our reconstruction using dual-axis tilt tomography. Unfortunately, since no threshold criterion was specified for the resolution value given in [15], this value cannot be used for an objective comparison. Besides dual-axis tomography, the presence of a unique, large additional A domain, close to the top of the F_1 headpiece in *Polytomella* (Fig. 4A), is probably beneficial in getting better alignments and thus in gaining higher resolution in averaged subvolumes. Other ET studies, like those on ribosomal distribution within intact mitochondria are also based on single-axis tilt series [7,8]. In one of the few examples of dual-axis cryo-ET, protein adhesion to liposomes was studied [30].

In conclusion, dual-axis cryo-ET is a powerful tool to investigate intact organelles with a size of around 1 μm, such as *Polytomella* mitochondria, and to retrieve structural details of the largest protein associations such as the OXPHOS supercomplexes. Previously, ET work was sometimes performed on very elongated objects, such as the *S. melliferum* cells studied by Ortiz and colleagues [7]. The reason to work with thin objects is obvious, because there is a direct relation between the diameter of the investigated object and the obtained resolution by ET [6]. The work presented here shows that it is possible to work with close-to-spherical intact mitochondria. But ET is not yet at its limits and a further increase in resolution on intact organelles is possible by implementing improved hardware. Next expansions are expected with the introduction of a new generation of cameras. Due to intrinsic multiple electron scattering within the phosphor, spatial resolution in CCD cameras is limited, especially at higher acceleration voltages used in cryo-ET. Consequently, new electronic detectors are needed based on more direct detection, thus avoiding the intermediate light conversion step required for CCDs [31]. It is expected that with improved hardware ET will be able to precisely detect many more protein interactions in organelles on the level of large protein complexes.

Acknowledgements

N.V.D. is supported by a VENI grant from the Netherlands Organization for Scientific Research NWO. We thank D.N. Mastronarde (University of Colorado), R. Kouřil and W. Keegstra for discussion.

Appendix A. Supplementary data

Supplementary data associated with this article can be found, in the online version, at doi:10.1016/j.bbabio.2009.11.004.

References

[1] C.A. Mannella, M. Marko, P. Penczek, D. Barnard, J. Frank, The internal compartmentation of rat-liver mitochondria: tomographic study using the high-voltage transmission electron microscope, Microsc. Res. Tech. 27 (1994) 278–283.
[2] D. Nicastro, A.S. Frangakis, D. Typke, W. Baumeister, Cryo-electron tomography of Neurospora mitochondria, J. Struct. Biol. 129 (2000) 48–56.
[3] T.G. Frey, G.A. Perkins, M.H. Ellisman, Electron tomography of membrane-bound cellular organelles, Ann. Rev. Biophys. Biomol. Str. 35 (2006) 199–224.
[4] C.A. Mannella, Structure and dynamics of the mitochondrial inner membrane cristae, Biochim. Biophys. Acta 1763 (2006) 542–548.
[5] R. Rabl, V. Soubannier, R. Scholz, F. Vogel, N. Mendl, A. Vasiljev-Neumeyer, C. Körner, R. Jagasia, T. Keil, W. Baumeister, M. Cyrklaff, W. Neupert, A.S. Reichert, Formation of cristae and crista junctions in mitochondria depends on antagonism between Fcj1 and Su e/g, J. Cell Biol. 185 (2009) 1047–1063.
[6] R.A. Crowther, D.J. DeRosier, A. Klug, Reconstruction of a three-dimensional structure from projections and its application to electron microscopy, Proc. R. Soc. Lond. A 317 (1970) 319–340.
[7] J.O. Ortiz, F. Förster, J. Kürner, A. Linaroudis, W. Baumeister, Mapping 70S ribosomes in intact cells by cryoelectron tomography and pattern recognition, J. Struct. Biol. 156 (2006) 334–341.
[8] F. Brandt, S.A. Etchells, J.O. Ortiz, A.H. Elcock, F.U. Hartl, W. Baumeister, The native 3D organization of bacterial polysomes, Cell 136 (2009) 261–271.
[9] I. Arnold, K. Pfeiffer, W. Neupert, R.A. Stuart, H. Schägger, Yeast mitochondrial F_1F_0-ATP synthase exists as a dimer: identification of three dimer-specific subunits, EMBO J. 17 (1998) 7170–7178.
[10] F. Minauro-Sanmiguel, S. Wilkens, J.J. García, Structure of dimeric mitochondrial ATP synthase: novel F_0 bridging features and the structural basis of mitochondrial cristae biogenesis, Proc. Natl. Acad. Sci. U. S. A. 102 (2005) 12356–12358.
[11] N.V. Dudkina, J. Heinemeyer, W. Keegstra, E.J. Boekema, H.P. Braun, Structure of dimeric ATP synthase from mitochondria: an angular association of monomers induces the strong curvature of the inner membrane, FEBS Lett. 579 (2005) 5769–5772.
[12] N.V. Dudkina, S. Sunderhaus, H.P. Braun, E.J. Boekema, Characterization of dimeric ATP synthase and cristae membrane ultrastructure from *Saccharomyces* and *Polytomella* mitochondria, FEBS Lett. 580 (2006) 3427–3432.

[13] F. Krause, N.H. Reifschneider, S. Goto, N.A. Dencher, Active oligomeric ATP synthases in mammalian mitochondria, Biochem. Biophys. Res. Commun. 329 (2005) 583–590.
[14] R.D. Allen, C.C. Schroeder, A.K. Fok, An investigation of mitochondrial inner membranes by rapid-freeze deep-etch techniques, J. Cell Biol. 108 (1989) 2233–2240.
[15] M. Strauss, G. Hofhaus, R.R. Schröder, W. Kühlbrandt, Dimer ribbons of ATP synthase shape the inner mitochondrial membrane, EMBO J. 27 (2008) 1154–1160.
[16] J.P. Abrahams, A.G. Leslie, R. Lutter, J.E. Walker, Structure at 2.8 Å resolution of F_1-ATPase from bovine heart mitochondria, Nature 370 (1994) 621–628.
[17] D. Stock, C. Gibbons, I. Arechaga, A.G. Leslie, J.E. Walker, The rotary mechanism of ATP synthase, Curr. Opin. Struct. Biol. 10 (2000) 672–679.
[18] M. Vázquez-Acevedo, P. Cardol, A. Cano-Estrada, M. Lapaille, C. Remacle, D. González-Halphen, The mitochondrial ATP synthase of chlorophycean algae contains eight subunits of unknown origin involved in the formation of an atypical stator-stalk and in the dimerization of the complex, J. Bioenerg. Biomembr. 38 (2006) 271–282.
[19] C.V. Iancu, E.R. Wright, J. Benjamin, W.F. Tivol, D.P. Dias, G.E. Murphy, R. Morrison, J.B. Heymann, G.J. Jensen, A "flip-flop" rotation stage for routine dual-axis electron cryotomography, J. Struct. Biol. 151 (2005) 288–297.
[20] J.R. Kremer, D.N. Mastronarde, J.R. McIntosh, Computer visualization of three-dimensional image data using IMOD, J. Struct. Biol. 116 (1996) 71–76.
[21] A.S. Frangakis, R. Hegerl, Noise reduction in electron tomographic reconstructions using nonlinear anisotropic diffusion, J. Struct. Biol. 135 (2001) 239–250.
[22] M. Van Heel, G. Harauz, Resolution criteria for 3-dimensional reconstruction, Optik 73 (1986) 119–122.
[23] S.J. Ludtke, P.R. Baldwin, W. Chiu, EMAN: semiautomated software for high-resolution single-particle reconstructions, J. Struct. Biol. 128 (1999) 82–97.
[24] H. Schägger, G. von Jagow, Blue native electrophoresis for isolation of membrane protein complexes in enzymatically active form, Anal. Biochem. 199 (1991) 223–231.
[25] R. van Lis, G. Mendoza-Hernández, G. Groth, A. Atteia, New insights into the unique structure of the F0F1-ATP synthase from the chlamydomonad algae *Polytomella* sp. and *Chlamydomonas reinhardtii*, Plant Physiol. 144 (2007) 1190–1199.
[26] E.J. Boekema, H. van Roon, J.F.L van Breemen, J.P. Dekker, Supramolecular organization of photosystem II and its light-harvesting antenna in partially solubilized membranes, Eur. J. Biochem. 266 (1999) 444–452.
[27] W. Junge, Torque generation and elastic power transmission in the rotary F0F1-ATPase, Nature 459 (2009) 364–370.
[28] J.E. Walker, J.E. Dickenson, The peripheral stalk of the mitochondrial ATP synthase, Biochim. Biophys. Acta 1757 (2006) 286–296.
[29] N. Yeremenko, R. Kouřil, J.A. Ihalainen, S. D'Haene, N. van Oosterwijk, E.G. Andrizhiyevskaya, W. Keegstra, H.L. Dekker, M. Hagemann, E.J. Boekema, H.C.P. Matthijs, J.P. Dekker, Supramolecular organization and dual function of the IsiA chlorophyll-binding protein in cyanobacteria, Biochemistry 43 (2004) 10308–10313.
[30] Y.N. He, G.J. Jensen, P.J. Bjorkman, Cryo-electron tomography of homophilic adhesion mediated by the neural cell adhesion molecule L1, Structure 17 (2008) 460–471.
[31] A.R. Faruqi, R. Henderson, Electronic detectors for electron microscopy, Curr. Opin. Struct. Biol. 17 (2007) 49–555.